

Starch Biosynthesis in Guard Cells But Not in Mesophyll Cells Is Involved in CO₂-Induced Stomatal Closing^{1[OPEN]}

Tamar Azoulay-Shemer, Andisheh Bagheri, Cun Wang, Axxell Palomares, Aaron B. Stephan, Hans-Henning Kunz^{2*}, and Julian I. Schroeder*

Division of Biological Sciences, Section of Cell and Developmental Biology, Center for Food and Fuel for the 21st Century, University of California, San Diego, La Jolla, California 92093-0116

ORCID IDs: 0000-0002-4291-6901 (T.A.-S.); 0000-0003-1083-3981 (A.B.); 0000-0001-6975-0959 (C.W.); 0000-0002-1101-7559 (A.P.); 0000-0001-8000-0817 (H.-H.K.).

Starch metabolism is involved in stomatal movement regulation. However, it remains unknown whether starch-deficient mutants affect CO₂-induced stomatal closing and whether starch biosynthesis in guard cells and/or mesophyll cells is rate limiting for high CO₂-induced stomatal closing. Stomatal responses to [CO₂] shifts and CO₂ assimilation rates were compared in *Arabidopsis* (*Arabidopsis thaliana*) mutants that were either starch deficient in all plant tissues (ADP-Glc-pyrophosphorylase [ADGase]) or retain starch accumulation in guard cells but are starch deficient in mesophyll cells (plastidial phosphoglucose isomerase [pPGI]). *ADGase* mutants exhibited impaired CO₂-induced stomatal closure, but *pPGI* mutants did not, showing that starch biosynthesis in guard cells but not mesophyll functions in CO₂-induced stomatal closing. Nevertheless, starch-deficient *ADGase* mutant alleles exhibited partial CO₂ responses, pointing toward a starch biosynthesis-independent component of the response that is likely mediated by anion channels. Furthermore, whole-leaf CO₂ assimilation rates of both *ADGase* and *pPGI* mutants were lower upon shifts to high [CO₂], but only *ADGase* mutants caused impairments in CO₂-induced stomatal closing. These genetic analyses determine the roles of starch biosynthesis for high CO₂-induced stomatal closing.

Stomatal pores are formed by pairs of guard cell in the leaf epidermis and regulate the diffusion of CO₂ for photosynthetic carbon fixation and transpirational

water loss of plants. Stomatal apertures are regulated by physiological and environmental factors, such as abscisic acid, CO₂, ozone, drought, light, humidity, and pathogens (Vavasseur and Raghavendra, 2005; Kim et al., 2010; Murata et al., 2015). Intercellular CO₂ (*C_i*) in leaves regulates stomatal conductance (Mott, 1988). *C_i* levels are determined by respiration, mesophyll photosynthesis, stomatal conductance, and atmospheric [CO₂] (Lawson et al., 2014).

¹ This research was funded by a grant from the National Science Foundation (MCB1414339; J.I.S.) and in part by a grant from the National Institutes of Health (GM060396) to J.I.S. T.A.-S. received support from a postdoctoral fellowship from the US-Israel Binational Agricultural Research and Development Fund (BARD F1-446-11) and from the UCSD Frontiers of Innovation Scholars Program, and H.-H.K. was supported by a Human Frontier Science Program Long-Term fellowship and an Alexander von Humboldt Feodor Lynen fellowship.

² Present address: School of Biological Sciences, Washington State University, Pullman, WA 99164-4236.

* Address correspondence to henning.kunz@wsu.edu or jischroeder@ucsd.edu.

The author responsible for distribution of materials integral to the findings presented in this article in accordance with the policy described in the Instructions for Authors (www.plantphysiol.org) is: Julian I. Schroeder (jischroeder@ucsd.edu).

T.A.-S. performed most of the research, including starch imaging analyses, gas exchange analyses, stomatal movement analyses, data analyses, and figure preparation; A.B. performed stomatal movement analyses; A.P. also performed, reanalyzed, and confirmed stomatal aperture measurement data; C.W. did initial *aps1* experiments and repeated and confirmed mutant phenotypes by gas exchange analyses; A.B.S. performed statistical and kinetic analyses of gas exchange data; T.A.-S., H.-H.K., and J.I.S. designed the research and provided suggestions throughout the research and manuscript preparation; T.A.-S. and J.I.S. wrote the manuscript with input from other authors.

The continuous rise in atmospheric CO₂ levels (Keeling et al., 2011) produces an increase in intercellular leaf CO₂ levels (*C_i*) and induces a reduction of stomatal apertures on a global scale (Medlyn et al., 2001; Hetherington and Woodward, 2003; Frommer, 2010). These effects have profound impact on global CO₂ and water exchange of plants, leaf heat stress, plant water-use efficiency, and gas exchange for optimal yields (Sellers et al., 1997; LaDeau and Clark, 2001; Medlyn et al., 2001; Battisti and Naylor, 2009; Holden, 2009; Bishop et al., 2014, 2015). Significant progress has been made in unraveling fundamental genetic components of the CO₂ signaling machinery (Webb and Hetherington, 1997; Leymarie et al., 1998; Hashimoto et al., 2006; Young et al., 2006; Negi et al., 2008; Vahisalu et al., 2008; Hu et al., 2010; Xue et al., 2011; Merilo et al., 2013; Chater et al., 2015; Takahashi et al., 2015; Tian et al., 2015; Engineer et al., 2016; Wang et al., 2016; Yamamoto et al., 2016).

Carbon fixation primarily takes place in the mesophyll tissue and is the main source of carbohydrates in plants. Guard cells, which contain smaller and fewer chloroplasts (Allaway and Setterfi, 1972; Willmer and Fricker,

[OPEN] Articles can be viewed without a subscription.

www.plantphysiol.org/cgi/doi/10.1104/pp.15.01662

1996), contribute only 2 to 4% of the CO₂ assimilation rates compared to those of mesophyll cells (Outlaw and De Vlieghere-He, 2001). Studies support the notion that guard cells act as a carbon sink, importing carbon from mesophyll cells (Gotow et al., 1988; Tallman and Zeiger, 1988; Poffenroth et al., 1992; Talbott and Zeiger, 1996; Stadler et al., 2003; Kang et al., 2007; Lawson, 2009). Moreover, recent research has found that guard cell chlorophyll is not directly required for CO₂ control of stomatal closing but is required for turgor development of guard cells (Azoulay-Shemer et al., 2015). However, since even these chlorophyll-deficient guard cells had significant starch levels (Azoulay-Shemer et al., 2015), the relative contribution of starch synthesis to CO₂-induced stomatal closing could not be determined.

Starch represents an end product of CO₂ fixation in plant cells and accumulates in both mesophyll and guard cells. Starch metabolism in guard cells was previously shown to be involved in stomatal opening in response to blue light (Ogawa et al., 1978; Tallman and Zeiger, 1988; Poffenroth et al., 1992; Talbott and Zeiger, 1993; Lasceve et al., 1997; Horrer et al., 2016), low CO₂-mediated stomatal opening (Outlaw and Manchester, 1979), and abscisic acid and drought (Dittrich and Raschke, 1977; Prasch et al., 2015). During stomatal opening, starch in guard cells is catabolized first into sugars (Outlaw, 1982; Poffenroth et al., 1992; Talbott and Zeiger, 1993; Ritte and Raschke, 2003). Malate is a metabolite that is derived from sugar metabolism as well from the photosynthetic product triose-phosphate, which is produced in guard cell chloroplasts, exported to the cytoplasm, and then metabolized to malate among additional products. The important role of malate as a counter ion for potassium accumulation during stomatal opening (Willmer and Dittrich, 1974; Outlaw and Manchester, 1979; Heldt and Piechulla, 2011; Lawson et al., 2014) is well established, and its metabolism is suggested to be involved in stomatal conductance regulation (Penfield et al., 2012). Based on measurements of K⁺ levels in guard cells using K⁺-sensitive microelectrodes, it has been suggested that potassium and its counterion malate alone cannot provide sufficient osmotic potential required to support stomatal opening (MacRobbie and Lettau, 1980). Sugars, from starch breakdown or imported from the mesophyll, were proposed to provide an additional osmoticum for stomatal opening (Talbott and Zeiger, 1993).

During stomatal closure, malate is removed from guard cells via gluconeogenesis-mediated starch synthesis (Schnabl, 1980) and via malate efflux from guard cells (Dittrich and Raschke, 1977; Van Kirk and Raschke, 1978). Furthermore, malate efflux via guard cell anion channels (Keller et al., 1989) and the resulting extracellular malate stimulates anion channel activity, which further promotes stomatal closing (Hedrich and Marten, 1993; Hedrich et al., 1994; Meyer et al., 2010). A comparison between *Vicia faba* and *Allium porrum* revealed that stomata of these species were generally

similar in their ultrastructure, except that *A. porrum* did not contain starch (Allaway and Setterfi, 1972). Metabolic investigation revealed that *A. porrum* guard cells use Cl⁻ rather than malate as counter ion to K⁺ (Schnabl, 1980; Schnabl and Raschke, 1980). In addition, comparative proteomics between guard cells and mesophyll cells revealed high representation of starch synthesis proteins in mesophyll cells but not in guard cells (Zhu et al., 2009). The relative contribution of starch metabolism in guard cells versus mesophyll cells in stomatal responses to CO₂ (Messinger et al., 2006; Mott et al., 2008) remains to be determined.

Starch levels in guard cells have been shown in biochemical studies to contribute to stomatal opening (Schnabl et al., 1978; Outlaw and Manchester, 1979; Schnabl, 1980; Talbott and Zeiger, 1993). In line with this model, starch degradation in guard cells was recently shown to contribute to light-induced stomatal opening. The *bam1 amy3* double mutant, which overaccumulates starch specifically in guard cells, showed reduced stomatal apertures and slower increases in stomatal conductance in response to light (Horrer et al., 2016). However, genetic analyses of the functions of starch biosynthesis in stomatal closing are lacking and the roles of starch biosynthesis in high CO₂-induced stomatal closing remain unknown. Based on present knowledge, it would be difficult to predict whether starch synthesis is required for intact CO₂-induced stomatal closing of preopened stomatal pores, as efflux of chloride and malate anions from guard cells occurs (Schnabl, 1980; Schnabl and Raschke, 1980; Keller et al., 1989).

Previous studies have characterized several starch-deficient mutants in the starch biosynthesis pathway. Independent allelic loss-of-function mutations in the small catalytic subunit of ADP-Glc-pyrophosphorylase (ADGase; *adg1-1* and *aps1*) were found to be starch deficient in all plant tissues (Lin et al., 1988; Wang et al., 1998; Bahaji et al., 2011). While the loss of the plastidial phosphoglucose isomerase (pPGI) activity (*pgi1-1* mutant) results in a starch-deficient phenotype in photoautotrophic tissues, in particular in the mesophyll, whereas guard cells have been shown to contain similar starch levels as wild-type controls (Yu et al., 2000; Tsai et al., 2009; Kunz et al., 2010). This phenomenon was attributed to the action of the Glc 6-phosphate/phosphate translocator (Overlach et al., 1993) that supplies the plastids of guard cells and of nongreen tissue with starch precursors, thereby circumventing the need for the plastidial phosphoglucose isomerase reaction (Kammerer et al., 1998; Niewiadomski et al., 2005).

To clarify whether and to what degree biosynthesis of starch in guard cells and/or mesophyll cells is required for high CO₂-induced stomatal closing, *Arabidopsis* (*Arabidopsis thaliana*) mutants that are either starch deficient in all plant tissues (ADGase mutants; *adg1-1* and *aps1*) or feature a specific starch-deficient phenotype in the mesophyll cells but not guard cells (*pgi1-1*) were compared for their stomatal responses to [CO₂].

RESULTS

Differential Starch Accumulation in *ADGase* and *pPGI* Mutants

Previously published data have demonstrated that *adg1-1* mutant plants, deficient in the small subunit of the starch biosynthesis enzyme ADGase, possess <3% of the wild-type ADGase activity (Lin et al., 1988; Wang et al., 1998) and accumulate as little as 1 to 2% of wild-type starch levels in leaves (Bahaji et al., 2011). The loss of pPGI activity in the *pgi1-1* mutant results in a lack of starch in the photoautotrophic mesophyll tissues of plants (Yu et al., 2000), but guard cells retain starch levels similar to wild-type controls (Tsai et al., 2009; Kunz et al., 2010). To verify these earlier determined spatial starch accumulation impairments of *ADGase* and *pPGI* mutants under our growth conditions, Col-0 (wild type), the two *ADGase* mutants *adg1-1* (Lin et al., 1988) and *aps1* (Ventriglia et al., 2008), and *pgi1-1* (Yu et al., 2000) were iodine-stained and imaged for their starch content. The results, obtained in our experiments, confirmed a drastic reduction in rosette leaf starch levels of both *ADGase* (*adg1-1* and *aps1*) and *pgi1-1* mutants compared to wild-type plants (Fig. 1, A–D). Further detailed microscopy analyses using the 5th true leaf of plants showed that starch granules were not clearly detectable in mesophyll cells of both the *adg1-1*, *aps1*, and *pgi1-1* mutants in contrast to wild-type leaves (Fig. 1, E–H). Furthermore, starch in guard cells was not detectable in the *ADGase* mutant plants (*adg1-1* and *aps1*; Fig. 1, K and L). In contrast, *pgi1-1* mutant leaves accumulated starch in guard cells to a similar extent as wild-type leaves (Fig. 1, I and J). These results are consistent

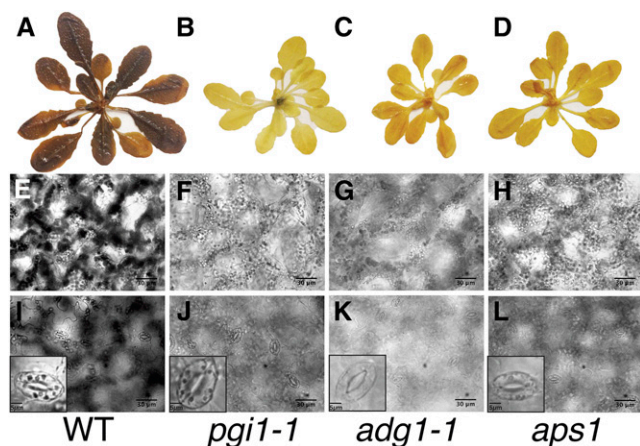


Figure 1. *ADGase* mutant (*adg1-1* and *aps1*) leaves show starch deficiency in both mesophyll and guard cells, whereas *pgi1-1* mutants accumulate starch in guard cells but not in mesophyll cells. Col-0, *ADGase* (*adg1-1* and *aps1*; Lin et al., 1988; Ventriglia et al., 2008), and *pPGI* (*pgi1-1*) mutants (Yu et al., 2000) were stained with iodine and imaged to visualize their starch content in whole plants (A–D), mesophyll (E–H), and guard cells (I–L). Bars in E to L = 30 μm (lower right) and in I to L = 5 μm (lower left).

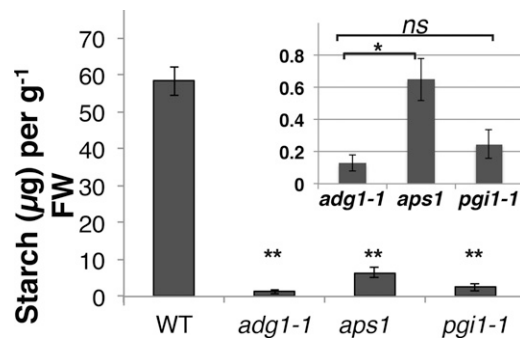


Figure 2. Leaf starch content in the *ADGase* and *pgi1-1* starch biosynthesis mutants. Rosettes from 6-week-old plants were harvested 2 h after the beginning of the light period and immediately frozen in liquid nitrogen. Starch was extracted and quantified using amylase/amyloglucosidase method. Unpaired Student's *t* test investigating statistical significance between mutants and the wild type showed a significant reduction in rosette leaf starch levels of *adg1-1*, *aps1*, and *pgi1-1* mutant plants (** $P \leq 0.005$, wild type, $n = 3$; *adg1-1*, $n = 4$; *aps1*, $n = 4$ and *pgi1-1*, $n = 4$; leaves, each leaf from different plant). Each bar shows the mean of wild type, *adg1-1*, *aps1*, or *pgi1-1* starch ($\mu\text{g} \pm \text{SE}$). Inset shows the same mutant data with a magnified y axis (starch [μg]/gFW). Student's *t* test between the starch-deficient mutants (*adg1-1*, *aps1*, and *pgi1-1*) revealed no significant (ns) differences between *adg1-1* (*ADGase* allele) and *pgi1-1* ($P = 0.3$), while *aps1* (*ADGase* allele) starch levels were slightly but significantly larger than *adg1-1* (* $P = 0.02$).

with previous studies (Tsai et al., 2009; Kunz et al., 2010): *adg1-1* is uniformly starch deficient in mesophyll and guard cells, whereas *pgi1-1* is starch deficient in mesophyll cells but not guard cells.

To quantitate the levels of starch in the starch biosynthesis mutants, rosettes from 6-week-old plants were harvested 2 h after the beginning of the light period and immediately frozen in liquid nitrogen. Starch quantification using the amylase/amyloglucosidase method (Eliyahu et al., 2015) showed a drastic and significant reduction in rosette leaf starch levels of the *adg1-1*, *aps1*, and *pgi1-1* mutants compared to wild-type plants (Fig. 2). Starch levels were slightly but significantly higher in the *aps1* *ADGase* allele compared to the *adg1-1* allele (Fig. 2).

Arabidopsis *ADGase* Mutants, But Not *pPGI* Mutants, Show Impaired Stomatal Closure in Response to High CO_2

Stomatal densities of the *ADGase* and *pPGI* starch biosynthesis mutants were not significantly different from the wild type (16.4 ± 0.4 in the wild type; 15 ± 2.3 in *adg1-1*; and 16.4 ± 2.3 in *pgi1-1*; *adg1-1* versus the wild type, $P = 0.5$; *pgi1-1* versus the wild type, $P = 0.2$, $n = 4$ plants per genotype, unpaired Student's *t* test). Starch levels have been associated with stomatal opening in diverse species. However, the relevance of starch in preopened stomata for CO_2 -induced stomatal closing remains unknown and is not trivial to predict. To determine to which degree starch levels in guard cells and/or in mesophyll cells are involved in high

CO₂-induced stomatal closing, time-resolved stomatal conductance responses to [CO₂] shifts were measured in intact leaves of wild-type (Col-0), the two *ADGase* mutant alleles *adg1-1* (Lin et al., 1988) and *aps1* (Ventriglia et al., 2008), and in *pPGI* mutant (*pgi1-1*) leaves (Yu et al., 2000). Both *ADGase* mutant alleles showed impaired high CO₂-induced stomatal closure (Fig. 3, A, B, E, and F; Fig. 3B, *adg1-1* versus the wild type, $P = 0.05$; Fig. 3F, *aps1* versus the wild type, $P = 0.04$, $n = 4$ –5 plants per genotype,

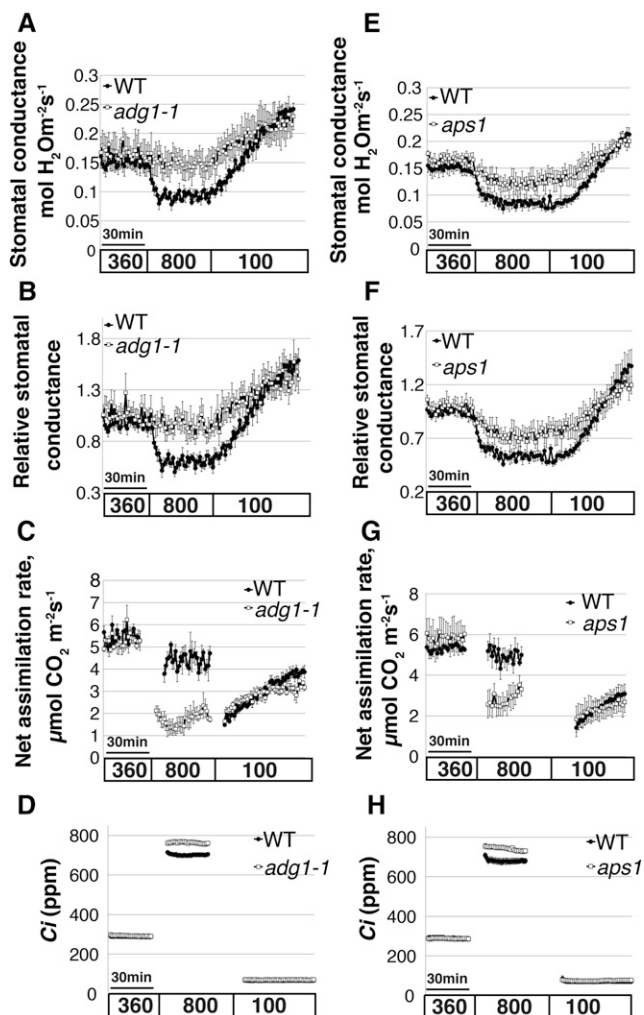


Figure 3. Arabidopsis starch-deficient *ADGase* mutants show impaired stomatal closure in response to CO₂ elevation. Time-resolved stomatal conductance responses and net CO₂ assimilation rates were analyzed at the imposed [CO₂] shifts (bottom in ppm) in the wild-type and in two starch-deficient *ADGase* Arabidopsis mutant alleles *adg1-1* (A–D) and *aps1* (E–H). A and E, Stomatal conductance in mol H₂O m⁻² s⁻¹. B and F, Data shown in A and E were normalized to the stomatal conductance after 25 min at 360 ppm [CO₂] exposure, 5 min before the change to 800 ppm [CO₂]. C and G, Net CO₂ assimilation rates (μmol CO₂ m⁻² s⁻¹). D and H, The corresponding intercellular [CO₂] (C_i) levels, calculated based on the stomatal conductance and ambient CO₂ concentration. Data are the mean of the wild type, $n = 4$, and *adg1-1*, $n = 4$ (A–D); wild type, $n = 5$, *aps1*, $n = 4$ (E–H) leaves each from different plants \pm SE for each genotype.

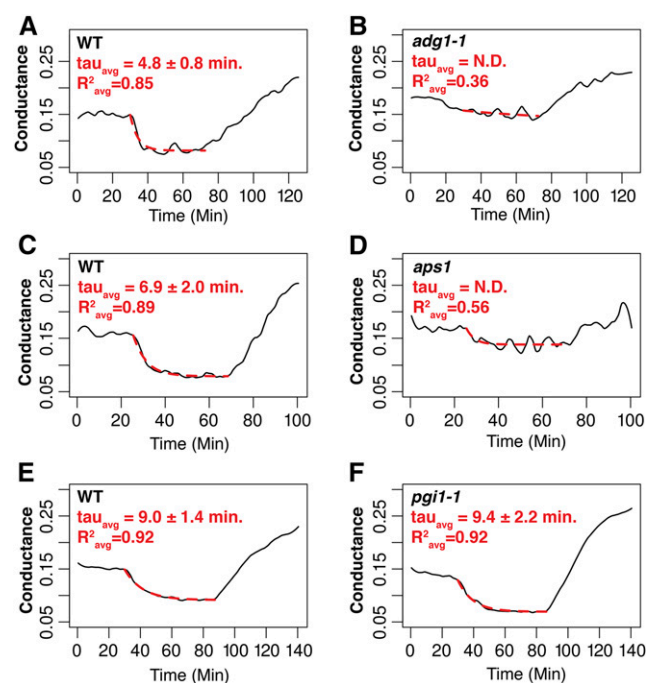


Figure 4. Analysis of CO₂-induced conductance kinetics. Single exponential functions were fit to data of high CO₂-induced stomatal closure (red dotted traces). A and B, Data traces and fits of wild-type Col-0 and *adg1-1* plants from within the same experiment. C and D, Data traces and fits of wild-type Col-0 and *aps1* plants from within the same experiment. E and F, Data traces and fits of wild-type Col-0 and *pgi1-1* plants from within the same experiment. R^2 values shown represent the average R^2 values for all leaves analyzed within the same experiment. The time constants displayed are means \pm SE of three to five plants.

unpaired Student's *t* test). Kinetic analyses, by fitting single exponential decay functions to the data, determined the time constant for stomatal closure in wild-type Col-0 (Fig. 4, A and C; $R^2_{avg} = 0.87$), but fitting the data of the *ADGase* mutants was not possible due to the small change in stomatal conductances (Fig. 4, B and D; $R^2_{avg} = 0.36$ for *adg1-1* and $R^2_{avg} = 0.56$ for *aps1*). Fits to the increases in stomatal conductance in response to low CO₂ (from 800 to 100 ppm CO₂) revealed that the stomatal opening rates of the *ADGase* mutant alleles were significantly smaller than the wild type (Fig. 3A, *adg1-1* versus the wild type, $P = 0.04$; Fig. 3E, *aps1* versus the wild type, $P = 0.05$).

Notably, although *ADGase* mutants are starch deficient in all plant tissues, including mesophyll and guard cells, a partial stomatal closure and opening in response to high CO₂ was observed (Fig. 3, E and F) in these mutant lines. The impairment in stomatal conductance responses to CO₂ in *ADGase* mutant alleles was comparable to other known and confirmed stomatal CO₂ response mutants (Hu et al., 2010; Xue et al., 2011; Merilo et al., 2013). Although steady-state stomatal conductance values differed at different times of year (Xu and Baldocchi, 2003), consistent

phenotypes and statistically significant differences in the high CO₂ response were observed when wild-type and *ADGase* mutant responses were compared within each set of plants and in independent replicates (see Methods).

CO₂ assimilation rate analyses showed a significant reduction in both starch-deficient *ADGase* mutant alleles (*adg1-1* and *aps1*) compared to those of the wild type under high CO₂ levels (800 ppm; Fig. 3C, $P = 7e-4$, *adg1-1* versus the wild type, $n = 4$; Fig. 3G, $P = 2e-2$, *aps1* versus the wild type, $n = 4-5$). However, under low CO₂ at photosynthesis-limiting conditions (100 ppm), no significant differences in CO₂ assimilation rates between the starch-deficient *ADGase* mutants and wild-type plants were observed (Fig. 3, C and G). A similar result was found if ambient CO₂ was clamped to 360 ppm. The corresponding intercellular [CO₂] (C_i) levels derived from stomatal conductance and CO₂ assimilation rates are shown in Figure 3, D and H.

Interestingly, stomatal conductance changes in *pgi1-1* mutant leaves (starch accumulation in guard cells, but not mesophyll cells) showed similar high CO₂-induced stomatal closing responses as wild-type plants upon shifting [CO₂] from ambient (360 ppm) to high (800 ppm) levels (Fig. 5, A and B; Fig. 5B, $P = 0.9$, $n = 3$, unpaired Student's *t* test). Furthermore, kinetic analysis determined no significant difference in the time constant for stomatal closure between the wild type and *pgi1-1* ($P = 0.86$, $R^2_{\text{avg}} = 0.92$ for the wild type, $R^2_{\text{avg}} = 0.92$ for *pgi1-1*; Fig. 4, E and F).

Intriguingly, the rate of the stomatal conductance increase in *pgi1-1* leaves following transition from a high (800 ppm) CO₂ level to a low CO₂ (100 ppm) level displayed a significantly amplified stomatal opening response when compared to wild-type leaves (Fig. 5B, $P = 0.05$, the wild type versus *pgi1-1*). Leaves of *pgi1-1* plants consistently showed enhanced stomatal opening, following exposure to low [CO₂], when compared to wild-type leaves. This result was observed in separate experiments during different times of the year. To verify the link between this phenotype and the PGI1 enzyme activity, we attempted isolation of a second allele in the *PGI1* gene. However, the tested T-DNA insertion alleles were either (homozygous) lethal or did not sufficiently disrupt PGI1 function (Salk_043552 and Salk_015973). Thus, we could not ascertain whether the stomatal opening phenotype of *pgi1-1* leaves is due to mutation of the *PGI1* gene and future research will be needed to examine this observation. In this study, we focus on high CO₂-induced stomatal closing responses in the differential starch biosynthesis mutants.

Net CO₂ assimilation rates (A) and C_i levels were analyzed (Fig. 5, C and D). *pPGI* mutant (*pgi1-1*) leaves showed a similar effect on CO₂ assimilation as *ADGase* mutants. *pgi1-1* assimilation rates were significantly reduced, compared to wild-type levels, under high CO₂ levels (800 ppm; Fig. 5C, $P = 0.05$, $n = 3$ leaves per genotype were analyzed in independent plants), while the corresponding *pgi1-1* C_i levels increased (Fig. 5D).

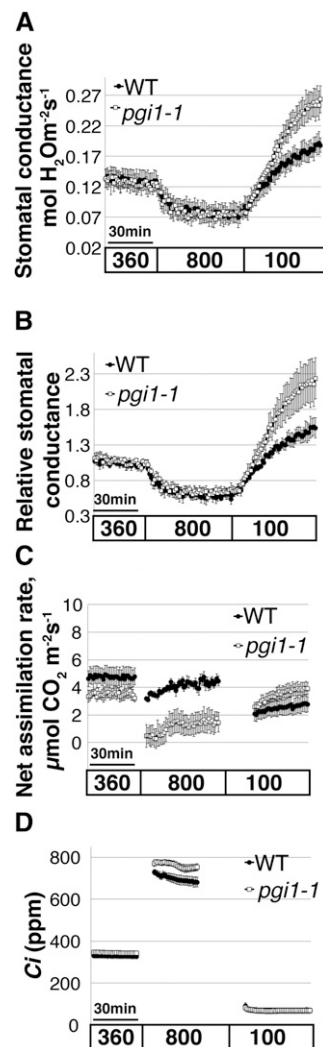


Figure 5. The *Arabidopsis pgi1-1* mutant that features starch deficiency in mesophyll cells but not in guard cells shows normal stomatal response to CO₂ elevation. Time-resolved stomatal conductance responses and net CO₂ assimilation rates at the imposed [CO₂] conditions (bottom in ppm) in the wild type and in the *Arabidopsis* starch-deficient mutant *pgi1-1* were analyzed using intact whole-leaf gas exchange. A, Stomatal conductance in mol H₂O m⁻² s⁻¹. B, Data shown in A were normalized to the stomatal conductance after 25 min of 360 ppm [CO₂] exposure, 5 min before the change to 800 ppm [CO₂]. C, CO₂ assimilation rates (μmol CO₂ m⁻² s⁻¹). D, The corresponding intercellular [CO₂] (C_i) levels, calculated based on the stomatal conductance and extracellular CO₂ concentration. Data in A to D are the mean of $n = 3$ leaves each from different plants \pm se for each genotype.

To further study stomatal responses at the single stoma level, the wild type and the starch-deficient mutants, *ADGase* (*adg1-1* and *aps1*) and *pPGI* (*pgi1-1*), were analyzed for their stomatal aperture responses to CO₂ elevation (Fig. 6), as described in “Materials and Methods.” Data in Figure 6, A to D, show that CO₂-induced stomatal closing in leaves of both *ADGase* mutant alleles was impaired (Fig. 6, A and B, wild type $P = 0.03$; *adg1-1* $P = 0.06$, $n = 3$ plants; Fig. 6, C and D,

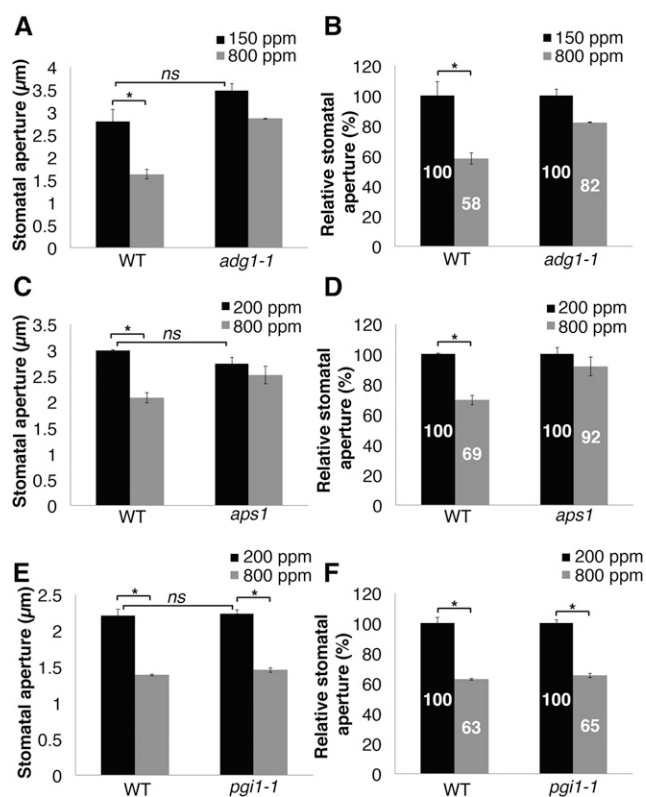


Figure 6. Stomatal aperture of the starch biosynthesis *ADGase* mutants show reduced response to CO₂ elevation but not *pgi1-1* mutant. Stomatal apertures in response to [CO₂] changes were measured in the wild type, the *ADGase* mutants *adg1-1* (A and B) and *aps1* (C and D), and in the *pPGI* mutant *pgi1-1* (E and F). B, D, and F, Relative stomatal apertures (%) for each genotype were calculated by normalization to the average stomatal apertures at low CO₂. A to F, Genotype blind assays, $n = 3$ plants per each genotype and treatment, ~ 135 stomata (A and B) and ~ 45 stomata (C–F) were analyzed per genotype and condition. Asterisks on the histograms indicate that the means differ significantly ($P \leq 0.05$), whereas “ns” indicates no significant difference ($P > 0.1$).

wild type $P = 0.008$; *aps1* $P = 0.35$, $n = 3$ plants). Wild-type stomatal apertures were reduced by ~ 30 to 42%, whereas those of *ADGase* mutant plants were reduced by ~ 8 to 18% (Fig. 6, B and C). In contrast, stomata of wild-type plants and *pgi1-1* mutant leaves, which are starch deficient in mesophyll but retain starch accumulation in guard cells, responded significantly to [CO₂] shifts (Fig. 6, E and F, wild type and *pgi1-1* $P < 0.02$, $n = 3$ plants per genotype). Unpaired Student's *t* tests between stomatal apertures of wild-type and the starch-deficient mutant lines, under low CO₂ levels, showed comparable stomatal apertures. This result suggests that low CO₂-induced steady-state apertures were not affected by the deficiencies in starch biosynthesis in mesophyll cells (*pgi1-1*) or in guard cells (*ADGase* mutants) (Fig. 6A, wild type/*adg1-1* $P = 0.1$; Fig. 6C, wild type/*aps1* $P = 0.16$; Fig. 6E wild type/*pgi1-1* $P = 0.1$, $n = 3$ plants). However, note that the rates of stomatal opening were slowed in both *ADGase* mutant

alleles that are starch deficient in guard cells (Fig. 3, A, B, E, and F).

DISCUSSION

The presented results show that starch biosynthesis in guard cells is required for proper high CO₂-induced stomatal closure, whereas starch biosynthesis in mesophyll cells had little or no role in this process. Several factors may be involved in the impaired stomatal closing response of guard cell starch-deficient mutants. The lack of starch biosynthesis as a sink for Calvin-Benson cycle CO₂ assimilation products leads to changes in metabolites, including free sugars, hexose phosphates, triose phosphates, and sugar phosphates (Tobias et al., 1992; Sun et al., 1999; Ragel et al., 2013), which have been suggested to be involved in stomatal conductance regulation (Hedrich et al., 1985). Accumulation of triose-phosphate may shift carbohydrate flux toward export to the cytosol and sucrose (Suc) synthesis. Accumulation of soluble sugars, including Fru, Glc, and Suc, was previously detected in *aps1* (Ragel et al., 2013).

Suc was reported to play a role in guard cell osmoregulation (Talbot and Zeiger, 1998; Zeiger et al., 2002), and its breakdown products, Fru and Glc, are also involved in stomatal conductance regulation (Antunes et al., 2012). In addition, Suc catabolism within guard cells can provide carbon skeletons for organic acid production (Dittrich and Raschke, 1977; Daloso et al., 2015). Increased levels of Suc, Fru, and Glc in *ADGase* mutant guard cells, as were previously shown in whole leaf extracts (Ragel et al., 2013), could contribute to the observed impaired stomatal closure (Figs. 3 and 6).

The disruption of mesophyll starch synthesis in *pgi1* and *ADGase* mutant leaves causes accumulation of sugars in the mesophyll (Kunz et al., 2010; Ragel et al., 2013). However, we have found that *pPGI* mutant leaves showed intact stomatal closure to elevated CO₂, suggesting that mesophyll-derived sugars do not account for the impaired CO₂-induced stomatal closure observed in *ADGase* mutant plants.

Malate is involved in stomatal responses. Malate acts as an osmoregulator in guard cells to promote stomatal opening (Willmer and Dittrich, 1974; Outlaw and Manchester, 1979; Heldt and Piechulla, 2011; Lawson et al., 2014). In order for stomata to close efficiently, malate has to be reconverted into starch to lower the turgor pressure of guard cells. On the other hand, during CO₂-induced stomatal closing, malate efflux from guard cells and a rise in the apoplastic malate concentration (Van Kirk and Raschke, 1978; Hedrich et al., 1994) enhance stomatal closing (Hedrich and Marten, 1993) by activation of QUAC1-encoded R-type anion channels (Hedrich and Marten, 1993; Hedrich et al., 1994; Meyer et al., 2010). As malate is produced from starch in guard cells, a putative reduced malate content in *ADGase* mutant guard cells would reduce this response. Further investigations of guard cell malate concentrations in the *ADGase* and *pPGI* mutants could test this model.

Starch degradation in guard cells was previously shown in biochemical studies to be involved in stomatal opening (Ogawa et al., 1978; Outlaw and Manchester, 1979; Tallman and Zeiger, 1988; Poffenroth et al., 1992; Talbott and Zeiger, 1993; Lasceve et al., 1997). It would be predicted that in the absence of starch in guard cells of the *ADGase* mutant, the rate of stomatal opening would be reduced. Our data show that the rates of low CO₂-induce stomatal opening in both *ADGase* mutant alleles was significantly reduced when compared to the wild type (Fig. 3, A and E), which is consistent with this hypothesis.

Note that this study does not contradict the results from recent research suggesting that mesophyll tissues produce a diffusible signal (Fujita et al., 2013; Mott et al., 2014) that amplifies stomatal responses to CO₂ changes. However, this study suggests that this factor is not directly linked to mesophyll starch. Further research is needed to determine whether this mesophyll factor is constitutive or whether CO₂ rapidly enhances the concentration of the presently unidentified mesophyll factor.

Starch metabolism is related to photosynthetic processes and impacts many other physiological pathways in plants (Caspar et al., 1985; Lunn et al., 2006; Ragel et al., 2013). Here, we show that in response to a step change from ambient to high CO₂ levels, net CO₂ assimilation rates were not significantly affected in wild-type plants (Figs. 3, C and G, and 5C), while those of both mesophyll starch-deficient *ADGase* and *PGI* mutants were lower when compared to wild-type levels (Figs. 3, C and G, and 5C). Our results correlate with previous studies in which wild-type and *ADGase* mutant plants were found to exhibit little or no difference in net CO₂ assimilation rates at ambient CO₂; however, at high CO₂ levels, net CO₂ assimilation rates were significantly reduced in both *ADGase* and *pPGI1* mutant plants (Sun et al., 1999; Ragel et al., 2013; Bahaji et al., 2015). The mechanisms involved in the reduction in the net CO₂ assimilation rates of *ADGase* and *PGI* mutants may involve triose phosphate utilization limited photosynthesis, which occurs at high CO₂ (Makino and Mae, 1999). During photosynthesis, triose phosphates are generated and converted into starch (in chloroplasts) or exported into the cytosol and metabolized to Suc (Leegood, 1996). In both cases, inorganic phosphate is released and reused in photophosphorylation. However, when starch biosynthesis is blocked, triose phosphates are produced more rapidly than they are consumed, causing shortage in the chloroplast inorganic phosphate pool, which limits photophosphorylation (Sharkey, 1985; Leegood and Furbank, 1986; Sharkey et al., 1986; Von Caemmerer, 2000). In wild-type *Arabidopsis* plants, the ratio of triose phosphate conversion to starch and Suc was higher under high CO₂ versus ambient CO₂ levels (Sun et al., 1999). This model is in line with our results, showing reduced net CO₂ assimilation rates in the starch biosynthesis mutants (*ADGase* and *pgi1-1*) but not in wild-type plants, following an increase in CO₂ above ambient levels (360

to 800 ppm; Figs. 3, C and G, and 5C). Interestingly, *ADGase* and *pPGI* also showed severalfold higher soluble sugar levels than wild-type plants (Kunz et al., 2010; Ragel et al., 2013), suggesting that the inhibition of CO₂ assimilation may be related to the metabolism and overaccumulation of soluble sugars (Goldschmidt and Huber, 1992).

Investigation of whole-leaf starch levels in the starch-deficient mutants revealed no significant differences between *adg1-1* and *pgi1-1*. However, although starch levels of the *aps1* (starch-deficient *ADGase* allele) were extremely low, statistical analysis found them to be significantly higher than those of the second *ADGase* allele, *adg1-1* (Fig. 2). Interestingly, whole-leaf net CO₂ assimilation rates at high CO₂ were impaired in *adg1-1* and *pgi1-1* to the same extent (Figs. 3C and 5C).

The role of photosynthesis in stomatal conductance regulation has been a matter of debate for many years (Lawson et al., 2014). Our results show that whole-leaf CO₂ assimilation rates upon transition to high CO₂ were impaired in both *pgi1-1* and *ADGase* mutants (Figs. 3, C and G, and 5C). However, CO₂-induced stomatal closure, in response to high CO₂ transition, was only impaired in *ADGase* mutants. On the other hand, *pgi1-1* mutant leaves showed a full stomatal closing response, following high CO₂ exposure (Figs. 5, A and B, and 6, E and F), even though this mutant is starch-deficient in mesophyll tissues (Yu et al., 2000; Figs. 1 and 2). These results correlate with the hypothesis that whole leaf photosynthesis is not the major mediator of CO₂ control of stomatal closing (Fig. 5). Our findings correlate with previous research suggesting that mesophyll photosynthesis is not a direct transducer of CO₂-regulated stomatal movements (Yu et al., 2000; von Caemmerer et al., 2004; Roelfsema et al., 2006). Our investigation does not strictly exclude a partial contribution of mesophyll photosynthesis, as we did not fully inhibit photosynthesis, which has been done in other research (Roelfsema et al., 2006).

Intercellular CO₂ (*C_i*) levels were slightly higher in both starch-deficient mutants *ADGase* (*adg-1* and *aps1*) and *pPGI* (*pgi1-1*) at high CO₂ levels (Figs. 3, D and H, and 5D). This increase in *C_i* is derived from the reduction in net CO₂ assimilation (Figs. 3, C and G, and 5C). Reduction in CO₂ assimilation by the Calvin-Benson cycle would result in an increase in *C_i*. Nevertheless, even these higher *C_i* levels in *ADGase* mutants did not induce wild-type-like stomatal high CO₂ responses (Figs. 3 and 5).

Furthermore, the finding that with only 1 to 2% of wild-type starch levels in *ADGase* mutant leaves (Bahaji et al., 2011) partial CO₂ responses occurred (Figs. 3, E and F, and 6A) suggests that a partial stomatal response to CO₂ elevation does not require fully active starch metabolism. Chloride ions have been previously shown to partially replace malate ions during stomatal regulation and may account for this weak starch-independent CO₂ response (Schnabl and Raschke, 1980).

In conclusion, these analyses of tissue-specific starch accumulation mutants quantify the relative function of

guard cell and mesophyll starch in CO₂-induced stomatal closing. While guard cell starch functions in high CO₂-induced stomatal closing, mesophyll starch and altered whole-leaf assimilation rates in starch biosynthesis mutants did not affect high CO₂-induced stomatal closing.

MATERIALS AND METHODS

Plant Material and Growth Conditions

For all investigations, the *Arabidopsis thaliana* accession Columbia (Col-0) was used as wild-type control and the following mutant alleles were investigated: two alleles of the small subunit of ADGase *ADG1* (AT5G48300), the EMS mutation *adg1-1* and the exon T-DNA insertion *aps1* (SALK_040155), and the pPGEI EMS mutation *pgi1-1*. T-DNA insertion lines *aps1* (SALK_040155) of the SALK were obtained from the ABRC. T-DNA insertion mutants were screened for homozygous individuals carrying a T-DNA insertion using the following primers: ADG LP, 5'-AACATTTCTCTAATGIGTGT-TATTCATG-3'; ADG RP, 5'-ACACACAGCCGCTTATTAC-3'; and left border primer LBa1 5'-TGGTTCACGTAGTGGCCATCG-3'.

All plant lines were cultivated on 0.5× MS medium (Murashige and Skoog, 1962) plus 0.8% (w/v) phyto agar and 0.8% (w/v) Suc. Seeds were stratified for 2 d at 4°C. Plants were grown in a Conviron growth chamber at a 12/12 h, 21°C/19°C day/night cycle, a photosynthetic photon flux density of ~110 μmol m⁻² s⁻¹, and 60 to 80% humidity. Ten-day-old seedlings were transferred to soil (Sunshine Professional Blending) and watered every 3 d to avoid water stress.

Starch Stain Analyses

The 5th true leaves of 29-d-old *Arabidopsis* plants were harvested at the end of the light cycle (12/12 h light cycle), decolorized with hot 80% (v/v) ethanol at 80°C, subsequently stained with Lugol's solution for 30 min, and then washed with double-distilled water three times, each time for 1 h. Whole-leaf preparations were then imaged using an inverted confocal Zeiss LSM 710 microscope. Bright-field images of stomata and the mesophyll were recorded. Data and image analysis was done with Image J (NIH; <http://rsbweb.nih.gov/ij/>).

Starch Quantification Analysis

Rosette leaf samples (100 mg) of 6 week-old plants were harvested 2 h after the beginning of the light period (12/12 h light cycle). Starch content was analyzed using the Sigma-Aldrich starch assay kit (SA20-1KT).

Time-Resolved CO₂-Dependent Intact Leaf Stomatal Conductance Measurements

Stomatal conductance was recorded from the 5th true leaf, from intact mature rosette nonsenescent 4- to 5.5-week-old plants. Recordings started 5 to 8 h after light cycle begin, using a Li-6400 infrared (IRGA)-based gas exchange analyzer system with a fluorometer chamber (Li-Cor). The following conditions were held in the measurement chamber: Relative humidity was held between 59 and 61%, temperature at 21°C, and photon flux density was 150 μmol m⁻² s⁻¹ (10% blue). Following gas exchange measurements, the analyzed leaf area was measured, calculated, and used in data analyses. Therefore, all calculated data are dependent on the stomatal density and the stomatal aperture responses within the chamber. As observed in previous studies, biological variation of steady-state baseline stomatal conductance occurs in *Arabidopsis* among plants grown at different times. Therefore, in all experiments, wild-type and mutant plants were grown side by side and analyzed in the same time period. Furthermore, all gas exchange experiments were repeated in at least three independent experimental sets at different times of the year. In each independent experimental data set, *n* ≥ 3 leaves per genotype were analyzed and representative data from one experimental data set are shown in each figure panel.

Stomatal responses to [CO₂] shifts were conducted as follows: Stomatal conductance was stabilized at 360 ppm [CO₂] for 30 min. Next, [CO₂] was shifted to 800 ppm for 45 min then changed to 100 ppm for 60 min. Data presented are means ± SE. For each genotype, data of three to five leaves (as indicated in figures) were averaged. Each leaf was the 5th true leaf from a

different plant. Relative stomatal conductance was calculated by normalization of each stomatal conductance to the stomatal conductance at 360 ppm [CO₂] immediately prior to the transition to 800 ppm [CO₂]. The number of biological repeats (*n* = number of plants) and stomata that were analyzed in each sample are indicated in the figure legends. Statistical analyses were done using unpaired Student's *t* tests between each transgenic line and parallel grown wild-type controls. Sample number (*n*) used in statistical analyses corresponded to the independent biological repeats of plants that were investigated for each line.

Unpaired Student's *t* tests between wild-type and mutant lines were done by comparing averaged stomatal conductance of the last 10 min (50 to 60 min) of 800 ppm exposure. Unpaired Student's *t* test between wild-type and mutant lines were done by comparing averaged net CO₂ assimilation rates over a period of 10 min (15–25 min) after transition to 800 ppm exposure. Pairwise Student's *t* test between net CO₂ assimilation rates of the wild type under ambient CO₂ and high CO₂ was done by comparison the averaged CO₂ assimilation rate of the first 30 min of 360 ppm exposure to 10 min (40–50 min) of 800 ppm exposure (Fig. 5C).

Estimates of [C_i] (μmol CO₂ mol air⁻¹) were calculated based on equations (von Caemmerer and Farquhar, 1981) by the Li-Cor analyzer system as described in the Li-6400 manual for full definition of parameters.

Note that the Li-6400 gas exchange analyzer was regularly calibrated and was zeroed before every gas exchange experiment. In addition, experiments in Figures 3 and 5 were repeated with an independent Li-6400XT gas exchange analyzer, showing consistent results.

Analysis of CO₂-Induced Conductance Kinetics

Time-resolved Li-Cor measurements were analyzed to quantify the kinetics of conductance changes in response to elevated and lowered CO₂ concentrations. To reduce high-frequency noise in the recordings, the raw, non-normalized data were filtered in R with the loess function, weight 0.1 (R Development Core Team, 2013). The segment of the recording for high CO₂-induced stomatal conductance reduction was fit with the single exponential function

$$G_i = e^{(-\text{time}_i/\tau)} * (G_{\text{start}} - G_{\text{asymptote}}) + G_{\text{asymptote}}$$

where *G* is the stomatal conductance, and the two fit parameters were the time constant *tau* and the conductance asymptote.

Stomatal Aperture Measurements

Stomatal movement analyses in response to [CO₂] were performed as follows: Plants were grown under ambient CO₂ levels for 4 weeks in a controlled growth chamber (21°C, 60–80% humidity with a 12-h-light/12-h-dark photoperiod regime at ~100 μmol m⁻² s⁻¹). For these analyses, plants were then moved to CO₂-controlled growth chambers (Percival; at 21°C, 60 to 80% humidity with ~100 μmol m⁻² s⁻¹ white light) and exposed to low [CO₂] (150 ppm for 2 h, Fig. 6, A and B; 200 ppm for 5 h, Fig. 6, C–F). Leaf epidermis was then extracted immediately and stomatal apertures were analyzed. For high CO₂-induced stomatal closing, intact plants that were also preincubated in low CO₂ in the same growth chamber, were then transferred to an identical high [CO₂] growth chamber (800 ppm for 1 h, Fig. 6, A and B; 800 ppm for 45 min, Fig. 6, C to F). Epidermis was then extracted immediately and stomatal apertures were analyzed. In Figure 6, A and B, epidermis extraction was done as follows: The abaxial side of leaves was gently pressed onto a coverslip with a thin coating of medical adhesive (Hollister). The upper cell layers were carefully removed using a razor blade. The leaf epidermis was then tenderly washed with a soft sponge and CO₂ equilibrated (150/800 ppm) water to remove any remaining mesophyll cells. The resulting epidermal fragments were imaged within 2 to 5 min to measure stomatal apertures with a digital camera attached to a microscope (BH2; Olympus). All experiments shown in Figure 6 were performed as genotype blind experiments. In Figure 6, A and B, *n* = 3 plants per each genotype and treatment. In each plant, the 5th leaf was sampled and a total of ~135 stomata were analyzed per condition. In Figure 6, C to F, *n* = 3, and in each plant the 4th and 5th leaf was sampled and a total of ~45 stomata were analyzed per condition.

Stomatal Index Analyses in True Leaf

Epidermis was extracted from the fifth true rosette leaves of 4- to 5-week-old *Arabidopsis* plants immediately after leaves were analyzed by the Li-Cor gas exchange analyzer. Leaf epidermis extraction was done as previously described

(in "Stomatal Aperture Measurements") using medical adhesive. The resulting epidermal fragments were imaged at 20 magnification with a digital camera attached to a microscope (BH2). Data analysis of stomatal density images was performed as genotype blind samples, $n = 3$ plants per each genotype, and in each plant the 5th leaf was sampled and a total of 14 images were taken and analyzed. Stomata and epidermal cells were manually counted for all images using the Cell Counter in Image J (NIH; <http://rsbweb.nih.gov/ij/>). Stomatal density was calculated by dividing the number of stomata to total epidermal cell number.

Accession Numbers

Sequence data of the loci investigated in this study can be found in the Arabidopsis Information Resource under the following accession numbers: At4g24620 (pPGI1) and At5g48300 (ADG1).

ACKNOWLEDGMENTS

We thank Markus Gierth, University of Cologne, Germany, for providing the *adg1-1* and *pgi1-1* seeds and Mark Estelle (UCSD, San Diego, CA) for access to the Zeiss LSM 710 confocal microscope.

Received October 30, 2015; accepted April 19, 2016; published April 21, 2016.

LITERATURE CITED

- Allaway WG, Setterfi G (1972) Ultrastructural observations on guard cells of *Vicia faba* and *Allium porrum*. *Can J Bot* **50**: 1405
- Antunes WC, Provart NJ, Williams TCR, Loureiro ME (2012) Changes in stomatal function and water use efficiency in potato plants with altered sucrolytic activity. *Plant Cell Environ* **35**: 747–759
- Azoulay-Shemer T, Palomares A, Bagheri A, Israelsson-Nordstrom M, Engineer CB, Bargmann BO, Stephan AB, Schroeder JI (2015) Guard cell photosynthesis is critical for stomatal turgor production, yet does not directly mediate CO₂- and ABA-induced stomatal closing. *Plant J* **83**: 567–581
- Bahaji A, Li J, Ovecka M, Ezquer I, Muñoz FJ, Baroja-Fernández E, Romero JM, Almagro G, Montero M, Hidalgo M, Sesma MT, Pozueta-Romero J (2011) *Arabidopsis thaliana* mutants lacking ADP-glucose pyrophosphorylase accumulate starch and wild-type ADP-glucose content: further evidence for the occurrence of important sources, other than ADP-glucose pyrophosphorylase, of ADP-glucose linked to leaf starch biosynthesis. *Plant Cell Physiol* **52**: 1162–1176
- Bahaji A, Sánchez-López AM, De Diego N, Muñoz FJ, Baroja-Fernández E, Li J, Ricarte-Bermejo A, Baslam M, Aranjuelo I, Almagro G, et al (2015) Plastidic phosphoglucose isomerase is an important determinant of starch accumulation in mesophyll cells, growth, photosynthetic capacity, and biosynthesis of plastidic cytokinins in *Arabidopsis*. *PLoS One* **10**: e0119641
- Battisti DS, Naylor RL (2009) Historical warnings of future food insecurity with unprecedented seasonal heat. *Science* **323**: 240–244
- Bishop KA, Betzelberger AM, Long SP, Ainsworth EA (2015) Is there potential to adapt soybean (*Glycine max* Merr.) to future [CO₂]? An analysis of the yield response of 18 genotypes in free-air CO₂ enrichment. *Plant Cell Environ* **38**: 1765–1774
- Bishop KA, Leakey ADB, Ainsworth EA (2014) How seasonal temperature or water inputs affect the relative response of C3 crops to elevated [CO₂]: a global analysis of open top chamber and free air CO₂ enrichment studies. *Food and Energy Security* **3**: 33–45
- Caspar T, Huber SC, Somerville C (1985) Alterations in growth, photosynthesis, and respiration in a starchless mutant of *Arabidopsis thaliana* (L.) deficient in chloroplast phosphoglucomutase activity. *Plant Physiol* **79**: 11–17
- Chater C, Peng K, Movahedi M, Dunn JA, Walker HJ, Liang YK, McLachlan DH, Casson S, Isner JC, Wilson I, et al (2015) Elevated CO₂-induced responses in stomata require ABA and ABA signaling. *Curr Biol* **25**: 2709–2716
- Daloso DM, Antunes WC, Pinheiro DP, Waquim JP, Araujo WL, Loureiro ME, Fernie AR, Williams TC (2015) Tobacco guard cells fix CO₂ by both Rubisco and PEPcase while sucrose acts as a substrate during light-induced stomatal opening. *Plant Cell Environ* **38**: 2353–2371
- Dittrich P, Raschke K (1977) Malate metabolism in isolated epidermis of *Commelina communis* L. in relation to stomatal functioning. *Planta* **134**: 77–81
- Eliyahu E, Rog I, Inbal D, Danon A (2015) ACHT4-driven oxidation of APS1 attenuates starch synthesis under low light intensity in Arabidopsis plants. *Proc Natl Acad Sci USA* **112**: 12876–12881
- Engineer CB, Hashimoto-Sugimoto M, Negi J, Israelsson-Nordström M, Azoulay-Shemer T, Rappel WJ, Iba K, Schroeder JI (2016) CO₂ sensing and CO₂ regulation of stomatal conductance: Advances and open questions. *Trends Plant Sci* **21**: 16–30
- Frommer WB (2010) Biochemistry. CO₂ common sense. *Science* **327**: 275–276
- Fujita T, Noguchi K, Terashima I (2013) Apoplastic mesophyll signals induce rapid stomatal responses to CO₂ in *Commelina communis*. *New Phytol* **199**: 395–406
- Goldschmidt EE, Huber SC (1992) Regulation of photosynthesis by end-product accumulation in leaves of plants storing starch, sucrose, and hexose sugars. *Plant Physiol* **99**: 1443–1448
- Gotow K, Taylor S, Zeiger E (1988) Photosynthetic carbon fixation in guard cell protoplasts of *Vicia faba* L.: Evidence from radiolabel experiments. *Plant Physiol* **86**: 700–705
- Hashimoto M, Negi J, Young J, Israelsson M, Schroeder JI, Iba K (2006) Arabidopsis HT1 kinase controls stomatal movements in response to CO₂. *Nat Cell Biol* **8**: 391–397
- Hedrich R, Marten I (1993) Malate-induced feedback regulation of plasma membrane anion channels could provide a CO₂ sensor to guard cells. *EMBO J* **12**: 897–901
- Hedrich R, Marten I, Lohse G, Dietrich P, Winter H, Lohaus G, Heldt HW (1994) Malate-sensitive anion channels enable guard-cells to sense changes in the ambient CO₂ concentration. *Plant J* **6**: 741–748
- Hedrich R, Raschke K, Stitt M (1985) A role for fructose 2,6-bisphosphate in regulating carbohydrate metabolism in guard cells. *Plant Physiol* **79**: 977–982
- Heldt H-W, Piechulla B (2011) 8 - Photosynthesis implies the consumption of water. In *Plant Biochemistry* (Fourth Edition). Academic Press, San Diego, pp 211–239
- Hetherington AM, Woodward FI (2003) The role of stomata in sensing and driving environmental change. *Nature* **424**: 901–908
- Holden C (2009) Climate change. Higher temperatures seen reducing global harvests. *Science* **323**: 193–193
- Horrer D, Flüttsch S, Pazmino D, Matthews JS, Thalmann M, Nigro A, Leonhardt N, Lawson T, Santelia D (2016) Blue light induces a distinct starch degradation pathway in guard cells for stomatal opening. *Curr Biol* **26**: 362–370
- Hu H, Boisson-Dernier A, Israelsson-Nordstrom M, Bohmer M, Xue S, Ries A, Godoski J, Kuhn JM, Schroeder JI (2010) Carbonic anhydrases are upstream regulators of CO₂-controlled stomatal movements in guard cells. *Nat Cell Biol* **12**: 87–93
- Kammerer B, Fischer K, Hilpert B, Schubert S, Gutensohn M, Weber A, Flüggé UI (1998) Molecular characterization of a carbon transporter in plastids from heterotrophic tissues: the glucose 6-phosphate/phosphate antiporter. *Plant Cell* **10**: 105–117
- Kang Y, Outlaw WH, Jr., Andersen PC, Fiore GB (2007) Guard-cell apoplastic sucrose concentration—a link between leaf photosynthesis and stomatal aperture size in the apoplastic phloem leader *Vicia faba* L. *Plant Cell Environ* **30**: 551–558
- Keeling CD, Piper SC, Whorf TP, Keeling RF (2011) Evolution of natural and anthropogenic fluxes of atmospheric CO₂ from 1957 to 2003. *Tellus B Chem Phys Meteorol* **63**: 1–22
- Keller BU, Hedrich R, Raschke K (1989) Voltage-dependent anion channels in the plasma membrane of guard cells. *Nature* **341**: 450–453
- Kim TH, Böhmer M, Hu H, Nishimura N, Schroeder JI (2010) Guard cell signal transduction network: advances in understanding abscisic acid, CO₂, and Ca²⁺ signaling. *Annu Rev Plant Biol* **61**: 561–591
- Kunz HH, Häusler RE, Fettke J, Herbst K, Niewiadomski P, Gierth M, Bell K, Steup M, Flüggé UI, Schneider A (2010) The role of plastidial glucose-6-phosphate/phosphate translocators in vegetative tissues of *Arabidopsis thaliana* mutants impaired in starch biosynthesis. *Plant Biol (Stuttg)* **12**(Suppl 1): 115–128
- LaDeau SL, Clark JS (2001) Rising CO₂ levels and the fecundity of forest trees. *Science* **292**: 95–98
- Laseve G, Leymarie J, Vavasseur A (1997) Alterations in light-induced stomatal opening in a starch-deficient mutant of *Arabidopsis thaliana* L. deficient in chloroplast phosphoglucomutase activity. *Plant Cell Environ* **20**: 350–358
- Lawson T (2009) Guard cell photosynthesis and stomatal function. *New Phytol* **181**: 13–34

- Lawson T, Simkin AJ, Kelly G, Granot D (2014) Mesophyll photosynthesis and guard cell metabolism impacts on stomatal behaviour. *New Phytol* **203**: 1064–1081
- Leegood RC (1996) Primary photosynthate production: physiology and metabolism. In E Zamski and AA Schaffer, eds, *Photoassimilate Distribution in Plants and Crops*. Marcel Dekker, New York, pp 21–42
- Leegood RC, Furbank RT (1986) Stimulation of photosynthesis by 2% oxygen at low temperatures is restored by phosphate. *Planta* **168**: 84–93
- Leymarie J, Vavasseur A, Lascève G (1998) CO₂ sensing in stomata of *abi1-1* and *abi2-1* mutants of *Arabidopsis thaliana*. *Plant Physiol Biochem* **36**: 539–543
- Lin TP, Caspar T, Somerville C, Preiss J (1988) Isolation and characterization of a starchless mutant of *Arabidopsis thaliana* (L.) Heynh lacking ADP-glucose pyrophosphorylase activity. *Plant Physiol* **86**: 1131–1135
- Lunn JE, Feil R, Hendriks JH, Gibon Y, Morcuende R, Osuna D, Scheible WR, Carillo P, Hajirezaei MR, Stitt M (2006) Sugar-induced increases in trehalose 6-phosphate are correlated with redox activation of ADP-glucose pyrophosphorylase and higher rates of starch synthesis in *Arabidopsis thaliana*. *Biochem J* **397**: 139–148
- MacRobbie EAC, Lettau J (1980) Potassium content and aperture in intact stomatal and epidermal cells of *Commelina communis* L. *J Membr Biol* **56**: 249–256
- Makino A, Mae T (1999) Photosynthesis and plant growth at elevated levels of CO₂. *Plant Cell Physiol* **40**: 999–1006
- Medlyn BE, Barton CVM, Broadmeadow MSJ, Ceulemans R, De Angelis P, Forstreuter M, Freeman M, Jackson SB, Kellomaki S, Laitai E, et al (2001) Stomatal conductance of forest species after long-term exposure to elevated CO₂ concentration: a synthesis. *New Phytol* **149**: 247–264
- Merilo E, Laanemets K, Hu H, Xue S, Jakobson L, Tulva I, Gonzalez-Guzman M, Rodriguez PL, Schroeder JI, Brosché M, Kollist H (2013) PYR/RCAR receptors contribute to ozone-, reduced air humidity-, darkness-, and CO₂-induced stomatal regulation. *Plant Physiol* **162**: 1652–1668
- Messinger SM, Buckley TN, Mott KA (2006) Evidence for involvement of photosynthetic processes in the stomatal response to CO₂. *Plant Physiol* **140**: 771–778
- Meyer S, Mumm P, Imes D, Endler A, Weder B, Al-Rasheid KA, Geiger D, Marten I, Martinoia E, Hedrich R (2010) AtALMT12 represents an R-type anion channel required for stomatal movement in *Arabidopsis* guard cells. *Plant J* **63**: 1054–1062
- Mott KA (1988) Do stomata respond to CO(2) concentrations other than intercellular? *Plant Physiol* **86**: 200–203
- Mott KA, Berg DG, Hunt SM, Peak D (2014) Is the signal from the mesophyll to the guard cells a vapour-phase ion? *Plant Cell Environ* **37**: 1184–1191
- Mott KA, Sibbersen ED, Shope JC (2008) The role of the mesophyll in stomatal responses to light and CO₂. *Plant Cell Environ* **31**: 1299–1306
- Murashige T, Skoog F (1962) A revised medium for rapid growth and bio assays with tobacco tissue cultures. *Physiol Plant* **15**: 473–497
- Murata Y, Mori IC, Munemasa S (2015) Diverse stomatal signaling and the signal integration mechanism. *Annu Rev Plant Biol* **66**: 369–392
- Negi J, Matsuda O, Nagasawa T, Oba Y, Takahashi H, Kawai-Yamada M, Uchimiya H, Hashimoto M, Iba K (2008) CO₂ regulator SLAC1 and its homologues are essential for anion homeostasis in plant cells. *Nature* **452**: 483–486
- Niewiadomski P, Knappe S, Geimer S, Fischer K, Schulz B, Unte US, Rosso MG, Ache P, Flügge UI, Schneider A (2005) The *Arabidopsis* plastidic glucose 6-phosphate/phosphate translocator GPT1 is essential for pollen maturation and embryo sac development. *Plant Cell* **17**: 760–775
- Ogawa T, Ishikawa H, Shimada K, Shibata K (1978) Synergistic action of red and blue light and action spectra for malate formation in guard cells of *Vicia faba* L. *Planta* **142**: 61–65
- Outlaw WH (1982) Carbon metabolism in guard cells. *Recent Adv Phytochem* **16**: 185–222
- Outlaw WH Jr, De Vlieghere-He X (2001) Transpiration rate. An important factor controlling the sucrose content of the guard cell apoplast of broad bean. *Plant Physiol* **126**: 1716–1724
- Outlaw WH, Manchester J (1979) Guard cell starch concentration quantitatively related to stomatal aperture. *Plant Physiol* **64**: 79–82
- Overlach S, Diekmann W, Raschke K (1993) Phosphate translocator of isolated guard cell chloroplasts from *Pisum sativum* L. transports glucose-6-phosphate. *Plant Physiol* **101**: 1201–1207
- Penfield S, Clements S, Bailey KJ, Gilday AD, Leegood RC, Gray JE, Graham IA (2012) Expression and manipulation of phosphoenolpyruvate carboxykinase 1 identifies a role for malate metabolism in stomatal closure. *Plant J* **69**: 679–688
- Poffenroth M, Green DB, Tallman G (1992) Sugar concentrations in guard cells of *Vicia faba* illuminated with red or blue light: Analysis by high performance liquid chromatography. *Plant Physiol* **98**: 1460–1471
- Prasch CM, Ott KV, Bauer H, Ache P, Hedrich R, Sonnewald U (2015) β -Amylase1 mutant *Arabidopsis* plants show improved drought tolerance due to reduced starch breakdown in guard cells. *J Exp Bot* **66**: 6059–6067
- R Development Core Team (2013) R: A Language and Environment for Statistical Computing. R Foundation for Statistical Computing, Vienna, Austria
- Ragel P, Streb S, Feil R, Sahrawy M, Annunziata MG, Lunn JE, Zeeman S, Mérida Á (2013) Loss of starch granule initiation has a deleterious effect on the growth of *Arabidopsis* plants due to an accumulation of ADP-glucose. *Plant Physiol* **163**: 75–85
- Ritte G, Raschke K (2003) Metabolite export of isolated guard cell chloroplasts of *Vicia faba*. *New Phytol* **159**: 195–202
- Roelfsema MR, Konrad KR, Marten H, Psaras GK, Hartung W, Hedrich R (2006) Guard cells in albino leaf patches do not respond to photosynthetically active radiation, but are sensitive to blue light, CO₂ and abscisic acid. *Plant Cell Environ* **29**: 1595–1605
- Schnabl H (1980) CO₂ and malate metabolism in starch-containing and starch-lacking guard-cell protoplasts. *Planta* **149**: 52–58
- Schnabl H, Bornman CH, Ziegler H (1978) Studies on isolated starch-containing (*Vicia faba*) and starch-deficient (*Allium cepa*) guard cell protoplasts. *Planta* **143**: 33–39
- Schnabl H, Raschke K (1980) Potassium chloride as stomatal osmoticum in *Allium cepa* L., a species devoid of starch in guard cells. *Plant Physiol* **65**: 88–93
- Sellers PJ, Dickinson RE, Randall DA, Betts AK, Hall FG, Berry JA, Collatz GJ, Denning AS, Mooney HA, Nobre CA, et al (1997) Modeling the exchanges of energy, water, and carbon between continents and the atmosphere. *Science* **275**: 502–509
- Sharkey T (1985) Photosynthesis in intact leaves of C₃ plants: Physics, physiology and rate limitations. *Bot Rev* **51**: 53–105
- Sharkey TD, Stitt M, Heineke D, Gerhardt R, Raschke K, Heldt HW (1986) Limitation of photosynthesis by carbon metabolism : II. O(2)-insensitive CO(2) uptake results from limitation of triose phosphate utilization. *Plant Physiol* **81**: 1123–1129
- Stadler R, Büttner M, Ache P, Hedrich R, Ivashikina N, Melzer M, Shearson SM, Smith SM, Sauer N (2003) Diurnal and light-regulated expression of AtSTP1 in guard cells of *Arabidopsis*. *Plant Physiol* **133**: 528–537
- Sun J, Okita TW, Edwards GE (1999) Modification of carbon partitioning, photosynthetic capacity, and O₂ sensitivity in *Arabidopsis* plants with low ADP-glucose pyrophosphorylase activity. *Plant Physiol* **119**: 267–276
- Takahashi S, Monda K, Negi J, Konishi F, Ishikawa S, Hashimoto-Sugimoto M, Goto N, Iba K (2015) Natural variation in stomatal responses to environmental changes among *Arabidopsis thaliana* ecotypes. *PLoS One* **10**: e0117449
- Talbott LD, Zeiger E (1993) Sugar and organic acid accumulation in guard cells of *Vicia faba* in response to red and blue light. *Plant Physiol* **102**: 1163–1169
- Talbott LD, Zeiger E (1996) Central roles for potassium and sucrose in guard-cell osmoregulation. *Plant Physiol* **111**: 1051–1057
- Talbott LD, Zeiger E (1998) The role of sucrose in guard cell osmoregulation. *J Exp Bot* **49**: 329–337
- Tallman G, Zeiger E (1988) Light quality and osmoregulation in vicia guard cells : evidence for involvement of three metabolic pathways. *Plant Physiol* **88**: 887–895
- Tian W, Hou CC, Ren ZJ, Pan YJ, Jia JJ, Zhang HW, Bai FL, Zhang P, Zhu HF, He YK, et al (2015) A molecular pathway for CO(2) response in *Arabidopsis* guard cells. *Nat Commun* **6**: 6057
- Tobias RB, Boyer CD, Shannon JC (1992) Alterations in carbohydrate intermediates in the endosperm of starch-deficient maize (*Zea mays* L.) genotypes. *Plant Physiol* **99**: 146–152
- Tsai HL, Lue WL, Lu KJ, Hsieh MH, Wang SM, Chen J (2009) Starch synthesis in *Arabidopsis* is achieved by spatial cotranscription of core starch metabolism genes. *Plant Physiol* **151**: 1582–1595

- Vahisalu T, Kollist H, Wang YF, Nishimura N, Chan WY, Valerio G, Lamminmäki A, Brosché M, Moldau H, Desikan R, Schroeder JI, Kangasjärvi J (2008) SLAC1 is required for plant guard cell S-type anion channel function in stomatal signalling. *Nature* **452**: 487–491
- Van Kirk CA, Raschke K (1978) Release of malate from epidermal strips during stomatal closure. *Plant Physiol* **61**: 474–475
- Vavasseur A, Raghavendra AS (2005) Guard cell metabolism and CO₂ sensing. *New Phytol* **165**: 665–682
- Ventriglia T, Kuhn ML, Ruiz MT, Ribeiro-Pedro M, Valverde F, Ballicora MA, Preiss J, Romero JM (2008) Two Arabidopsis ADP-glucose pyrophosphorylase large subunits (APL1 and APL2) are catalytic. *Plant Physiol* **148**: 65–76
- Von Caemmerer S (2000) *Biochemical Models of Leaf Photosynthesis*. CSIRO Publishing, Collingwood VIC, Australia
- von Caemmerer S, Farquhar GD (1981) Some relationships between the biochemistry of photosynthesis and the gas exchange of leaves. *Planta* **153**: 376–387
- von Caemmerer S, Lawson T, Oxborough K, Baker NR, Andrews TJ, Raines CA (2004) Stomatal conductance does not correlate with photosynthetic capacity in transgenic tobacco with reduced amounts of Rubisco. *J Exp Bot* **55**: 1157–1166
- Wang C, Hu H, Qin X, Zeise B, Xu D, Rappel WJ, Boron WF, Schroeder JI (2016) Reconstitution of CO₂ regulation of SLAC1 anion channel and function of CO₂-permeable PIP2;1 aquaporin as carbonic anhydrase 4 interactor. *Plant Cell* **28**: 568–582
- Wang SM, Lue WL, Yu TS, Long JH, Wang CN, Eimert K, Chen J (1998) Characterization of ADG1, an Arabidopsis locus encoding for ADPG pyrophosphorylase small subunit, demonstrates that the presence of the small subunit is required for large subunit stability. *Plant J* **13**: 63–70
- Webb AA, Hetherington AM (1997) Convergence of the abscisic acid, CO₂, and extracellular calcium signal transduction pathways in stomatal guard cells. *Plant Physiol* **114**: 1557–1560
- Willmer C, Fricker M (1996) *Topics in Plant Functional Biology*, 2. Stomata, Ed 2, Vol 2. Chapman & Hall, UK
- Willmer CM, Dittlich P (1974) Carbon dioxide fixation by epidermal and mesophyll tissues of Tulipa and Commelina. *Planta* **117**: 123–132
- Xu L, Baldocchi DD (2003) Seasonal trends in photosynthetic parameters and stomatal conductance of blue oak (*Quercus douglasii*) under prolonged summer drought and high temperature. *Tree Physiol* **23**: 865–877
- Xue S, Hu H, Ries A, Merilo E, Kollist H, Schroeder JI (2011) Central functions of bicarbonate in S-type anion channel activation and OST1 protein kinase in CO₂ signal transduction in guard cell. *EMBO J* **30**: 1645–1658
- Yamamoto Y, Negi J, Wang C, Isogai Y, Schroeder JI, Iba K (2016) The transmembrane region of guard cell SLAC1 channels perceives CO₂ signals via an ABA-independent pathway in Arabidopsis. *Plant Cell* **28**: 557–567
- Young JJ, Mehta S, Israelsson M, Godoski J, Grill E, Schroeder JI (2006) CO(2) signaling in guard cells: calcium sensitivity response modulation, a Ca(2+)-independent phase, and CO(2) insensitivity of the gca2 mutant. *Proc Natl Acad Sci USA* **103**: 7506–7511
- Yu TS, Lue WL, Wang SM, Chen J (2000) Mutation of Arabidopsis plastid phosphoglucose isomerase affects leaf starch synthesis and floral initiation. *Plant Physiol* **123**: 319–326
- Zeiger E, Talbott LD, Frechilla S, Srivastava A, Zhu JX (2002) The guard cell chloroplast: a perspective for the twenty-first century. *New Phytol* **153**: 415–424
- Zhu M, Dai S, McClung S, Yan X, Chen S (2009) Functional differentiation of *Brassica napus* guard cells and mesophyll cells revealed by comparative proteomics. *Mol Cell Proteomics* **8**: 752–766